Miniaturized Fractal Antenna Design for 6-GHz 5G Advanced Communications

Prabhat K. Patnaik[1], M. Murali[2], Harish C. Mohanta[1], and Dhruba C. Panda[3]
[1]Department of Electronics & Communication Engineering, Centurion University of Technology and Management, Odisha, India
[2]Department of Electronics & Communication Engineering, Centurion University of Technology and Management, Andhra Pradesh, India
[3]Department of Electronic Science, Berhampur University, Berhampur, India

Corresponding author: Prabhat K. Patnaik (e-mail: prabhat.ku.patnaik@gmail.com).

ABSTRACT In this article, a miniaturized, low-profile fractal antenna is designed and prototyped for 6-GHz n104 band 5G advanced communications. Antenna miniaturization is achieved here by considering the random Sierpinski fractal concept and optimizing the structure with the genetic algorithm. Initially, the proposed antenna is designed and optimized using Ansys HFSS. Subsequently, the performance of the antenna is also tested for different atmospheric conditions in MATLAB real-time simulation environment for advanced 5G applications in the presence of foliage and rain. The proposed antenna resonates at 6.5 GHz with an impedance bandwidth of 380 MHz and a gain of 5.21 dBi. The antenna has a low size of 0.39 λ_0 x 0.30 λ_0 with a size reduction of 76% compared to its conventional design, where λ_0 is the free space wavelength. The proposed low-profile antenna with balanced performance characteristics is found to be a suitable candidate for n104 band 5G advanced communications.

INDEX TERMS Advanced 5G Communication, Antenna Miniaturization, n104 Band, Optimization, Sierpinski Fractal.

I. INTRODUCTION

Nowadays, wireless communication technology demands high spectrum capacity to fulfill the requirement of broadband, IoT, data analysis, smartphones, and Industry 4.0. In addition to the available spectrums, more bands are dedicatedly required for 5G communications. To satisfy these criteria, most of the global telecom service providers are demanding 6 GHz band allocations for upcoming advanced 5G communications. This 6 GHz band is divided into two parts. The lower band from 5.9 GHz to 6.4 GHz is used in Wi-Fi applications. The upper 6 GHz band ranging from 6.425 GHz to 7.1 GHz is now standardized as 3GPP band n104 under WRC-23 discussions. Equipments for this band are in the testing phase now. This band has the capacity to meet all the demands of the customers with a bandwidth of 1 GHz. The addition of n104 band for advanced 5G communication will boost the communication network in terms of productivity and from a business point of view in the upcoming days. Selection of suitable transmitter and receiver antennas defines the robustness of a wireless network and the performance of the network depends purely on it. Low-cost, low-profile patch antennas are always on the radar of researchers for their compactness, reliability, and efficiency. Microstrip patch antennas (MPAs) also have the advantage in their design and performance over a wide range of frequency bands. The conventional MPAs still need miniaturization to satisfy the low space requirements for high-frequency portable communications.

Many antenna miniaturization techniques have already been investigated in the literature. Some of these methods include the use of shorting via [1], inductively loading of a cuboid ridge [2], using different fractal concepts [3], topology-based designs [4], use of meta-materials [5, 6], and split-ring resonator [7-10]. In 2012, split-ring resonators and reactive metasurfaces were used to design miniaturized microstrip antennas [6]. The antenna although exhibits a compact size, its performance is highly affected due to by very low gain. Later, in 2013, a topology-based antenna miniaturization technique was proposed [4]. The researchers were able to miniaturize a patch antenna using fractal concepts varying its iterations and indentations [3]. However, the volume of the above two designs [3, 4] was high compared to a conventional antenna. Even though in [1] and [2], the proposed MPAs are miniaturized to some extent with the use of shorting and cuboid ridge, both designs suffered from very low operating bandwidths. Defected ground structure is also a promising methodology in designing compact patch antennas [11-13]. Deliberately etching a portion of the ground plane of the microstrip antenna, the surface current patch length is increased to downshift the operating frequency of the antenna. The increase in the current flow path increases the effective electrical length of the patch. Ultimately, a decrease in operating frequency is observed with the same size of the patch. Many structures, like dumbbells [11],

circular strips [12], triangular shapes [13], etc., are been proposed for miniaturized patch designs. Although a good reduction in antenna size was achieved by these methods, the gain of the antenna is very low from an application point of view. Among other concepts, antenna miniaturization by fractal concept is also effective. The self-similar structure of fractal can shift antenna resonant frequencies. With the same dimensions, the microstrip antenna works at other frequencies due to the space-filling properties of the antenna. The conventional use of the fractal concept in antennas leads to a limited choice in antenna design. Hence, the application of the random fractal concept with genetic algorithm optimization is used here to explore the maximum utility of the proposed method.

In this article, a miniaturized, low-profile fractal antenna is designed and prototyped for 6-GHz n104 band 5G advanced communications. Antenna miniaturization is achieved here by considering the random Sierpinski fractal concept and optimizing the structure with a genetic algorithm. Initially, the proposed antenna is designed and optimized using Ansys HFSS. Subsequently, the antenna performance is tested for different atmospheric conditions in MATLAB real-time simulation environment for advanced 5G applications in the presence of foliage and rain. At first, a conventional proximity-coupled fed patch antenna is designed at 6.5 GHz. In the next step, another small-sized patch antenna is designed at a higher frequency and a random Sierpinski fractal with genetic algorithm is used to bring back its frequency to 6.5 GHz in Section II. Then, prototypes of both conventional antenna and miniaturized are fabricated in Section III. Both simulation and measured reflection and radiation characteristics are matched for both designs in the same section. In Section IV, the proposed miniaturized design was tested in MATLAB real-time simulation environment considering different atmospheric conditions. After comparing the proposed design in terms of its size and other performances with similar designs available, the article concluded in Section V.

II. MINIATURIZED ANTENNA DESIGN

This article mainly focuses on designing a compact microstrip antenna using a random fractal concept. As, the main aim of choosing n104 upper 6 GHz band is to accommodate a wider spectral capacity for advanced 5G communication, a dual-layered proximity coupled fed patch antenna is considered here. The conventional antenna (Design-1) is designed at fr = 6.5 GHz, and its geometry consists of a completely grounded dielectric substrate, a feed on the top of it, and another dielectric substrate with a radiating square patch at the top. The geometry of the proposed conventional patch antenna is shown in Figure 1. RO3003 with ϵ_r of 3 is taken as both upper- and lower-layer dielectric substrate. Later, another similar low-size dual-layered proximity coupled fed patch antenna (Design-2) is designed at a higher frequency of 10 GHz. The same RO3003 substrate is used in Design-2. Finally, a random Sierpinski fractal with iteration-2 is applied to Design-2 to bring back its resonant frequency to 6.5 GHz. The dimensions of Design-1 and Design-2 are given in Table I.

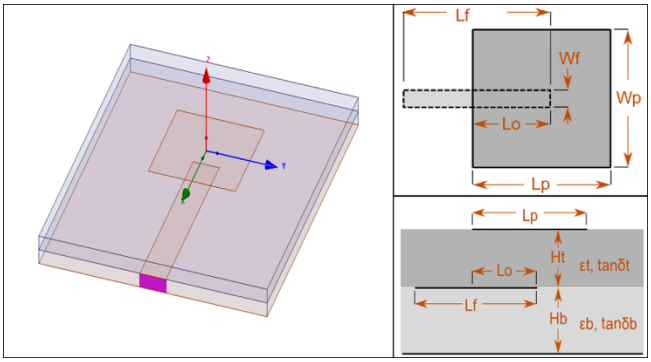

FIGURE 1. Dual-Layered Proximity Coupled Fed Antenna Design.

TABLE I. Antenna Dimensions

Design Parameters	Design-1 Values (mm)	Design-2 Values (mm)
Lp	11.3	7.9
Wp	11.3	7.9
Lo	5.594	3.72
Hb	1.52	0.51
Ht	1.52	0.51
Lf	20.66	11.16
Wf	3.381	1.18
Eb	3	3
Et	3	3
X-Total	35.486	18.4
Y-Total	29.54	14.02
Z-Total	3.04	1.02

At first, with the help of the following transmission line equations, for the operating frequency, ϵ_r, and height of the substrate material, the dimensions of the conventional proximity coupled patch antennas are designed for both 6.5 GHz and 10 GHz.

The width of the patch can be calculated from,

$$W = \frac{1}{2f_r\sqrt{\mu_0\epsilon_0}}\sqrt{\frac{2}{\epsilon_r+1}} \quad (1)$$

Substituting ϵ_r, h, and calculated W value in the following equation, the effective dielectric constant (ϵ_{reff}) and the extensive length (ΔL) are calculated.

$$\epsilon_{reff} = \frac{\epsilon_r+1}{2} + \frac{\epsilon_r-1}{2}\left[1+12\frac{h}{W}\right]^{-\frac{1}{2}} \quad (2)$$

$$\Delta L = 0.412h \frac{(\epsilon_{reff}+0.3)\left(\frac{W}{h}+0.264\right)}{(\epsilon_{reff}-0.258)\left(\frac{W}{h}+0.8\right)} \quad (3)$$

Now, the actual length (L) of the MPA is found by the following equation.

$$L = \frac{1}{2f_r\sqrt{\epsilon_{reff}}\sqrt{\mu_0\epsilon_0}} - 2\Delta L \quad (4)$$

As the width of the patch is much smaller than the operating wavelength, the input resistance at the edge (Rin(y=0)) of the patch can be evaluated from:

$$G_1 = \frac{1}{90}\left(\frac{W}{\lambda_0}\right)^2 for\ W \ll \lambda \quad (5)$$

$$R_{in}(y=0) = \frac{1}{2G_1} \quad (6)$$

The microstrip line must have the appropriate width to match the patch with the feed line. The width of the microstrip feed line (W_0) and the distance y_0 can be calculated by using following equations.

$$Z_0 = \frac{60}{\sqrt{\epsilon_{reff}}} ln\left[\frac{8h}{W_0} + \frac{W_0}{4h}\right] \quad (7)$$

$$R_{in}(y=y_0) = R_{in}(y=0)\cos^2\left(\frac{\pi}{L}\right)y_0 \quad (8)$$

In [14], Lamsalli et. al., have used a genetic algorithm to miniaturize antenna size up to 82%. They are able to bring back the resonating frequency of the antenna from 4.9 GHz to 2.16 GHz by dividing the whole design into 100 similar pieces. Considering this concept, to miniaturize the antenna at 6.5 GHz, another small antenna can be designed at a higher frequency of 15 GHz. For designing a patch antenna, the operating frequency, the effective dielectric constant of the substrate material, and its height play an important role. While reducing the resonating frequency of the miniaturized antenna from 10 GHz to 6.5 GHz, its operating wavelength increases. But, with the help of random Sierpinski fractal concept and genetic algorithm optimization, the patch structure is adjusted in such a way that, the antenna resonates at the desired frequency i.e. 6.5 GHz without hampering the effective dielectric constant and height of the substrate material. These two properties of the Substrate kept same as the conventional antenna to have a valid comparison in patch size miniaturization. Hence, we can choose a similar design at any frequency between 15 GHz and use this method to bring its operating frequency to 6.5 GHz. An antenna at 10 GHz with dual-layered proximity coupled feed is taken here instead of 15 GHz to avoid low gain due to the small size patch of the antenna. After, designing the proximity-fed antenna at 10 GHz proximity-fed antenna, a random fractal is applied based on the Sierpinski carpet fractal of the 2nd iteration. At first, the whole radiating element is divided into 81 patches with of Lp/9 and Wp/9 sizes. Then 17 patches with either 0 or 1 values are considered over these 81 patches to meet the design goal. A value of 0 indicates the absence of the conductor, while a value of 1 indicates its presence. In genetic algorithm optimization, an initial population is created and, in each iteration,, the algorithm uses the current population to create the next population. Positions of these 17 patches are determined through the optimization process of the structure, such that the evolved structure meets the design goal (Figure 2).

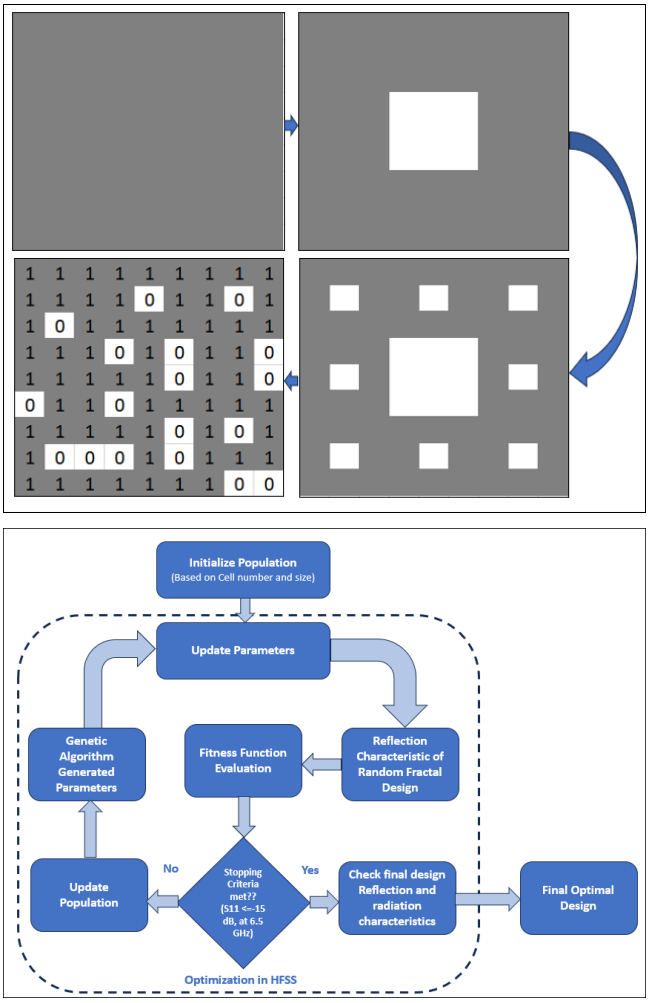

FIGURE 2. Random Sierpinski Fractal Design with Iteration-2 and genetic algorithm optimization process in HFSS.

At each iteration, based on the design, it calculates the S11 parameters and evaluates the objective function to meet the desired resonance value at 6.5 GHz. During optimization, designs that exhibit electrical discontinuity are discarded. The length and width of the feed were first designed to operate the antenna at 10 GHz. Hence, along with the optimization of the position and size of the patches, the length and width of the feed are also optimized at each iteration to provide maximum current flow to the radiating

patch by matching the impedance to 50 Ω. Finally, by optimizing the structure, the resonant frequency of the 10 GHz antenna shifts back to 6.5 GHz. The miniaturized antenna (0.39 λ_0 x 0.30 λ_0) has a 76% size reduction than the conventional 6.5 GHz antenna (0.76 λ_0 x 0.64 λ_0) without any degradation in the performance parameters of the antenna. Their resonant frequency can be observed from the S11 vs. frequency graph in Figure 3. From the same figure, it can be marked that both Design-1 and Design-2, now resonate around 6.5 GHz frequency, with impedance bandwidths of 450 MHz and 380 MHz, respectively.

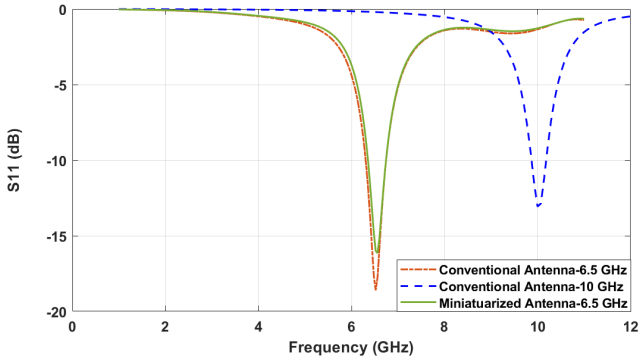

FIGURE 3. S11 Vs. Frequency plot of antenna designs.

The surface current distribution can be seen in Figure 4 for both Design-1 and Design-2 at 6.5 GHz. The difference in color represents the different magnitudes of surface current (Red-Max, Blue-Min). It can be observed from the figure that the surface current is distributed all over the surface area for both designs. By introducing perturbations at the patch with random fractal, the surface current distribution is altered, which results in generating resonating frequencies at a different band.

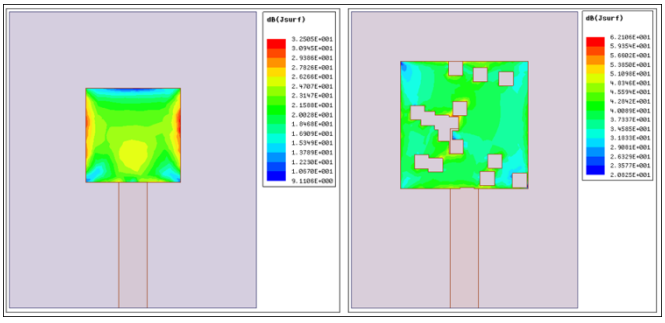

FIGURE 4. Surface current visualization of (a) Design-1, (b) Design-2, at 6.5 GHz.

III. RESULTS AND DISCUSSIONS

After the design and optimization of the proposed antenna, the miniaturized antenna along with the conventional one, is fabricated with same RO3003 substrate. A Windows® CPU @ 3.19 GHz system with 16 GB of RAM and 4 parallel cores system is used for the design and optimization of the antenna. Both reflection characteristics and radiation characteristics are then measured and compared with the simulated ones. The miniaturized antenna (18.4 mm x 14.02 mm) shows a 76% size reduction compared to the conventional 6.5 GHz antenna (35.48 mm x 29.54 mm), as shown in Figure 5.

The S11 characteristics of both designs are measured in an Agilent N5247A VNA. Figure 6 depicts both simulated and measured S11 results over a frequency range for both designs. From the same figure, it can be seen that, both the antenna prototypes resonate at 6.5 GHz while following the same trend as the simulated S11 curves. A minor variation among simulated and measured results was observed due to fabrication error at the feed point and joint of two substrate layers. The conventional and miniaturized antennas exhibit 10-dB return loss bandwidths of 450 MHz, and 380 MHz, respectively centered at 6.5 GHz.

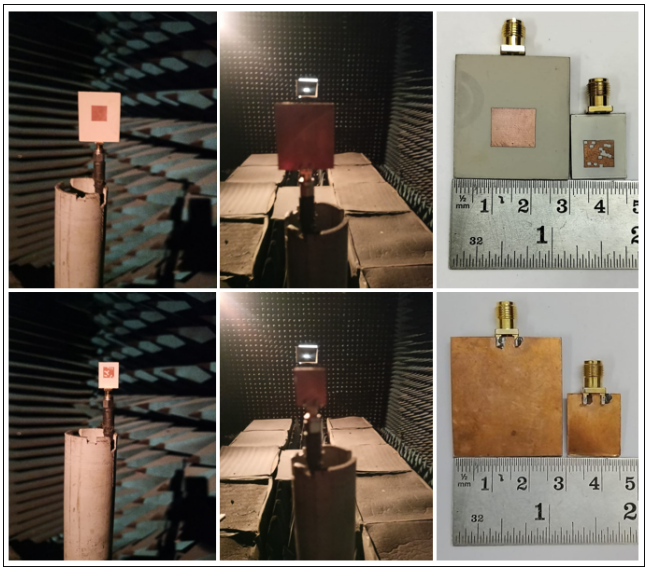

FIGURE 5. Conventional and Miniaturized antenna prototypes placed in an anechoic chamber with front and back views.

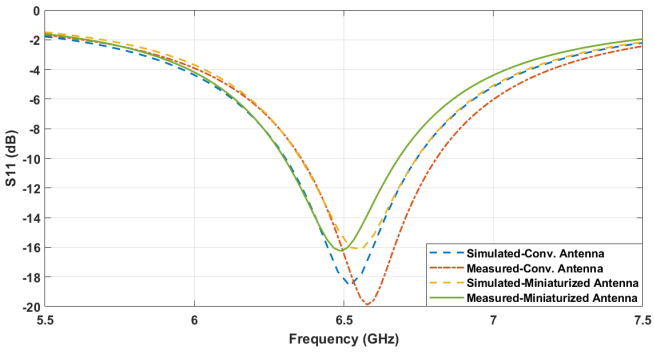

FIGURE 6. Simulated and measured S11 Vs. frequency for Design-1 and Design-2.

Both the fabricated designs are then kept in a standard anechoic chamber with a fully automated rotor for far-field radiation pattern measurement. Figure 5 portrays the

arrangements for both E-plane and H-plane radiation pattern measurements. A horn antenna is placed at the transmitter side, and the antenna prototypes are placed as AUT at the receiver side for their received power measurement. The simulated and measured radiation patterns for both Design-1 and Design-2 are figured for the E-plane (XZ-plane, $\phi = 0^0$) and H-plane (YZ-plane, $\phi = 90^0$) in Figure 7 (a) and (b), respectively. Both the simulated and measured radiation patterns agree with each other. The conventional design has a measured E-plane and H-plane gain of 7.13 dBi and 7.11 dBi, respectively at 6.5 GHz. Similarly, the miniaturized one has a measured gain of 5.21 dBi and 5.19 dBi for the E-plane and H-plane, respectively. It can also be observed from the figure that both designs generate a symmetric gain pattern in the E and H-planes. The proposed miniaturized design exhibits a minor asymmetry in the gain pattern due to perturbations in its radiating patch.

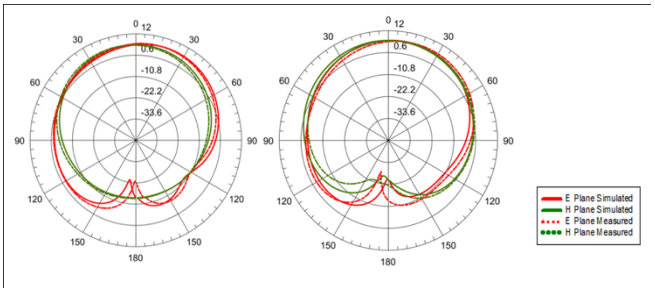

FIGURE 7. Simulated and measured radiation patterns for both E-Plane and H-Plane, (a) Conventional Antenna, (b) Miniaturized antenna.

After successful fabrication of the antenna prototype and matching the measured results with simulated ones, a comparison is carried out among the proposed designs and other similar designs reported in the literature. This comparison is required to validate the proposed method of antenna miniaturization and antenna performance parameters like gain and bandwidth. All the designs considered here for comparison are resonating at slightly different frequencies. Hence, to provide a valid comparison among all the antenna dimensions, the size of the antennas is compared here in terms of their operating wavelength. The antenna designs are also compared in terms of their operational bandwidth, percentage of size reduction, and antenna gain, as shown in Table II.

TABLE II. Performance comparison among proposed designs with other available designs

Antenna Design	Antenna Dimension	Size Reduction	Resonating Frequency (GHz)	Gain (dB)	Bandwidth (MHz)
Conventional Antenna	0.76 λ_0 x 0.64 λ_0	30%	6.5	7.13	450
[15], 2022	0.48 λ_0 x 0.40 λ_0	72%	5.2	6.21	836
[16], 2024	0.56 λ_0 x 0.56 λ_0	55%	6.5	4.26	810
[17], 2017	0.46 λ_0 x 0.49 λ_0	67%	4.5	5.24	180
[18], 2023 (Reference)	0.92 λ_0 x 0.76 λ_0	-	6	3.8	900
[19], 2023	0.33 λ_0 x 0.33 λ_0	84%	4.5	2.65	800
Proposed Miniaturized Antenna	0.39 λ_0 x 0.30 λ_0	83%	6.5	5.21	380

Among all, the design in [18], has a maximum dimension of 0.92 λ_0 x 0.76 λ_0, and is taken as a reference to evaluate the percentage of size reduction for other compared designs. The design in [19], has the maximum 84% size reduction compared to 83% in our case. However, the antenna has a very low gain of 2.65 dBi compared to 5.21 dBi of the proposed miniaturized antenna. Similarly, the antenna design in [15] has a maximum gain of 6.21 dBi, but the antenna has a 72% reduction in size. The antenna in [18] has a maximum of 900 MHz impedance bandwidth, but it has a very large antenna size with a very low gain of only 3.8 dBi. Although, the proposed miniaturized antenna is not the best among all in all cases, with a size reduction of 83%, gain of 5.21 dBi, and an impedance bandwidth of 380 MHz, it serves with the most balanced performance characteristics for the proposed advanced 5G communications.

IV. ANTENNA PERFORMANCE EVALUATION IN SIMULATION ENVIRONMENT

After the design and fabrication of the miniaturized antenna, the performance of the antenna needs to be tested in real-time environments. Single antenna integration and its testing in real-time is quite costly, difficult, and time-consuming. Hence, before bulk production of the design, it is first tested in real-time simulation scenarios encompassing all environmental factors. MATLAB provides similar test scenarios for the performance measurement of antennas. At first, the proposed miniaturized antenna is redesigned in MATLAB, and then its performance evaluation is carried out. It is ensured that the reflection characteristics (S11) and radiation characteristics (3D antenna gain) of the miniaturized antenna match each other in both the HFSS and MATLAB environments. Then, a custom antenna is created based on these imported data. Then, their 3D radiation patterns are matched to confirm the redesigned custom antenna in MATLAB. Figure 8 depicts the 3D radiation patterns of the proposed antennas for ANSYS HFSS and MATLAB. After the successful matching of 3D patterns, the custom antenna is now ready for its performance test in real-time simulation environment.

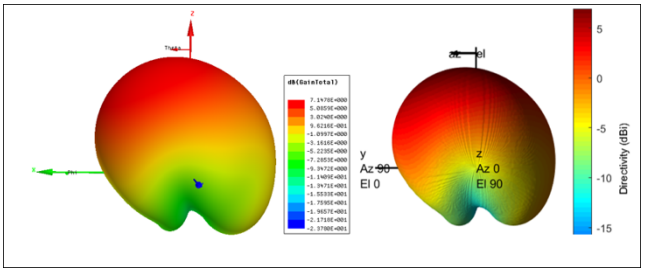

(a) (b)

FIGURE 8. 3D Radiation patterns of Miniaturized antenna in (a) HFSS, (b) MATLAB.

Now, a simulation environment is created in MATLAB with a transmitter and multiple receivers to look like a 5G advanced communication network. A single transmitter (Tx) with eight receivers (Rx) is created around it, with different angles, as seen in Figure 9. Then, the created custom antenna is attached to the Tx-site, which has a height of 60 m and a transmitter power of 15 dB. The transmitter frequency is kept at 6.5 GHz. The radiation pattern of the proposed antenna at Tx-site is depicted in Figure 10. Similarly, all eight receivers are created at different locations around the Tx, with a height of 10 m and a sensitivity of -90 dBm in satellite view.

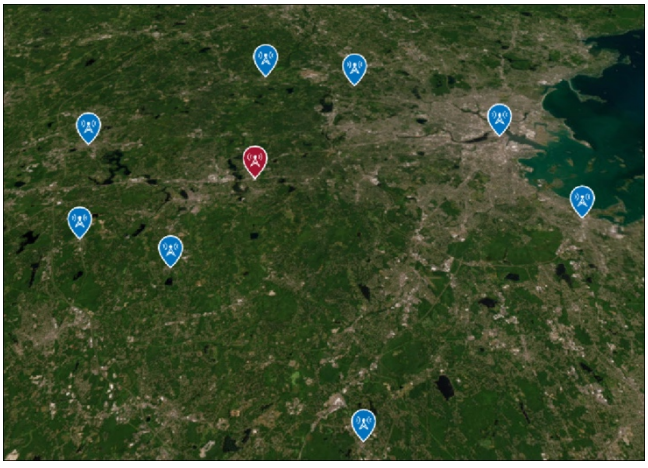

FIGURE 9. Satellite view of Tx and 8 Rx-Sites placed in a Map.

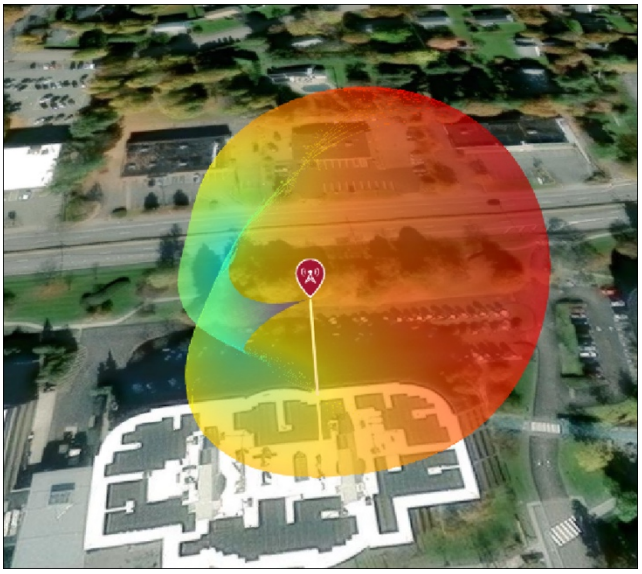

FIGURE 10. Antenna radiation pattern placed at Tx-Site.

After checking the radiation pattern at Tx-site, the coverage of the Tx antenna is then observed in Figure 11. The range of the transmitter antenna purely depends on the gain of the transmitter antenna and the input power given to it. Along with the input power of 15 dB, the single antenna gives a coverage of 500 m with a gain of 7 dB, and the transmitter antenna with an array has a range of up to 2000 m with a gain of 17 dB. Hence, while determining the range of the Tx, the single antenna has an overall range of 22 dB and the antenna array has 32 dB. A communication link is then tried to form among the Tx-site and all 8 Rx-sites. As per the coverage of the Tx-site, out of 8 Rx-sites, only 3 Rx-sites are able to be in a link with the Tx. The other 5 receivers couldn't establish a link with the Tx as they were not in the range of the Tx antenna.

Tx-site with a single sector at a particular angle cannot be able to provide coverage in all directions. Hence, 3 sectors are attached to the Tx-site with the same custom antenna in 3 different directions to accommodate all Rx-Sites. Now, with 3 sectors, a successful communication link is established between each Rx with the Tx as shown in Figure 12. All eight Rx-sites are now in the coverage of the Tx with a range from -70 dB to -90 dB.

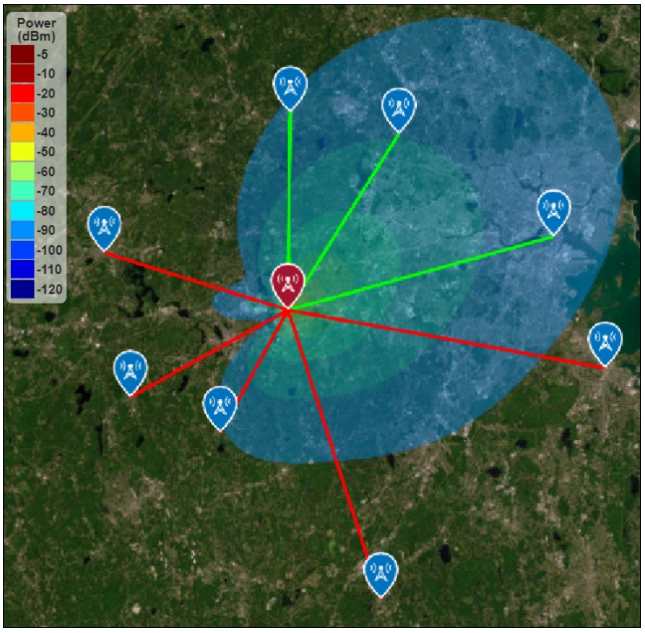

FIGURE 11. Tx-Site coverage Map link among Tx-Site and eight Receivers.

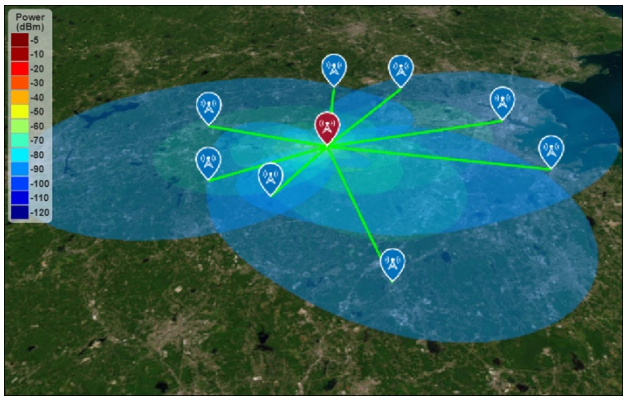

FIGURE 12. Tx-Site has three sectors at three different angles, and there is a successful communication link between Tx and all Rx-Sites.

Now, with all links among Tx and Rxs, the communication network is established. The performance of the proposed miniaturized antenna is evaluated with the communication network at 6.5 GHz. The proposed antenna is used here as a transmitter antenna, and its performance is evaluated based on the receiver signal strengths at all receivers in the presence of different environmental factors like rain, fog, and foliage blockages. The receiver signal strengths at all Rx-sites are compared in Table III in the presence of noises like foliage and rain. With a single antenna at all 3 Sectors of Tx-Site, the receiver signal strength varies between -80 dB to -90 dB. The loss due to 15 m foliage is found to be around 11 dB, and path loss due to combined 15 m foliage with 10 mm rain is around 24 dB with the given communication network. The receiver signal strength is now getting below -100 dBm with a combined loss due to rain and foliage. Hence, considering this signal strength below -100 dBm, the receivers will face call/data drops. To avoid this problem, a uniform rectangular array of size 8x8 is now installed at each sector of the transmitter site by taking the custom antenna from the individual element. The distance among the elements in the array is kept as $\lambda_0/2$ for both row and column-wise. The radiation pattern after installing the antenna array at Tx-site can be observed in Figure 13.

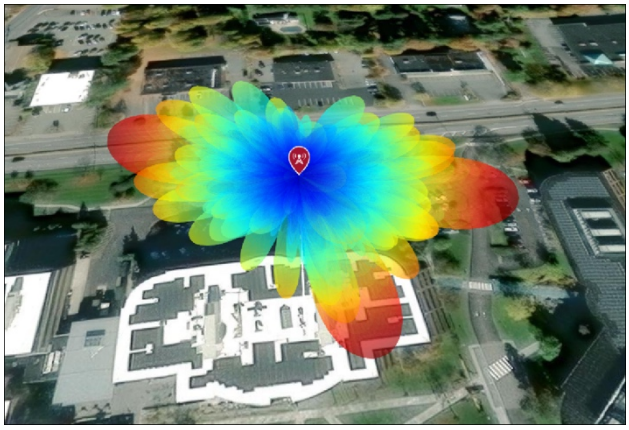

FIGURE 13. Uniform rectangular array radiation pattern at three sectors of the Tx-Site.

The gain of the antenna array is found to be 17 dB. Again, the receiver signal strength is measured at all Rxs with the same foliage and rain path losses. From Table III, the receiver signal strengths are found in the range of -70 dBm to -80 dBm without any losses, and with combined blockage of rain and foliage, the signal strength is below -100 dBm. This is the ideal case, with an antenna array at Tx-site, where the Rxs will not face any call or data drop issues. The proposed miniaturized antenna and its array are now successfully tested in MATLAB real-time simulation environment and exhibit a good communication network to its Rx-sites with all atmospheric losses.

TABLE III. Comparison of received signal strengths at each Rx-Sites with a single antenna and antenna array.

Receiver	Free Space		15 m Foliage Loss		15 m Foliage and 10 mm Rain	
Signal Strength (dBm)	Single Antenna	Antenna Array	Single Antenna	Antenna Array	Single Antenna	Antenna Array
Rx1	-85.89	-76.67	-97.24	-88.02	-106.36	-97.14
Rx2	-87.66	-78.44	-99.01	-89.79	-108.13	-98.91
Rx3	-88.24	-79.02	-99.59	-90.37	-108.71	-99.49
Rx4	-89.43	-80.21	-100.78	-91.56	-109.9	-100.68
Rx5	-87.69	-78.47	-99.04	-89.82	-108.16	-98.94
Rx6	-83.74	-74.52	-95.09	-85.87	-104.21	-94.99
Rx7	-83.41	-74.19	-94.76	-85.54	-103.88	-94.66
Rx8	-86.04	-76.82	-97.39	-88.17	-106.51	-97.29

This proves the feasibility of the proposed antenna for the 6-GHz 5G advanced communications with its compact size. The use of an antenna array also opens the possibility of

using array beamforming with much higher directivity towards the target Rx site without wasting power in the null zones.

VI. CONCLUSION

In this article, a miniaturized, low-profile fractal antenna is designed and prototyped for 6-GHz n104 band 5G advanced communications. Antenna miniaturization was achieved by considering the random Sierpinski fractal concept and optimizing the structure with a genetic algorithm. Initially, the proposed antenna is designed and optimized using HFSS. Subsequently, the performance of the antenna is tested for different atmospheric conditions in the MATLAB real-time simulation environment for advanced 5G applications in the presence of foliage and rain. The receiver signal strengths are measured and compared with a single antenna and antenna array to evaluate the performance of the proposed design in real harsh conditions. The proposed antenna exhibits a stable communication network and is found to be an ideal candidate for the 6 GHz 5G advanced communications. Further, there is a lot of scope available to exploit the use of antenna arrays in n104 band communication with other scenarios such as multi-transmitters and mobile receivers.

REFERENCES

[1] A. Boukarkar, X. Q. Lin, Y. Jiang, and Y. Q. Yu, "Miniaturized Single-Feed Multiband Patch Antennas," in IEEE Transactions on Antennas and Propagation, vol. 65, no. 2, pp. 850-854, Feb. 2017. (doi: 10.1109/TAP.2016.2632620)

[2] A. Motevasselian and W. G. Whittow, "Patch size reduction of rectangular microstrip antennas by means of a cuboid ridge," in IET Microwaves, Antennas & Propagation, vol. 9, no. 15, pp. 1727-1732, 12 10 2015. (doi: 10.1049/iet-map.2014.0559)

[3] V. V. Reddy and N. V. S. N. Sarma, "Compact Circularly Polarized Asymmetrical Fractal Boundary Microstrip Antenna for Wireless Applications," in IEEE Antennas and Wireless Propagation Letters, vol. 13, pp. 118-121, 2014. (doi: 10.1109/LAWP.2013.2296951)

[4] J. Oh and K. Sarabandi, "A Topology-Based Miniaturization of Circularly Polarized Patch Antennas," in IEEE Transactions on Antennas and Propagation, vol. 61, no. 3, pp. 1422-1426, March 2013. (doi: 10.1109/TAP.2012.2231915)

[5] H. X. Xu, G. M. Wang, J. G. Liang, M. Q. Qi and X. Gao, "Compact Circularly Polarized Antennas Combining Meta-Surfaces and Strong Space-Filling Meta-Resonators," in IEEE Transactions on Antennas and Propagation, vol. 61, no. 7, pp. 3442-3450, July 2013. (doi: 10.1109/TAP.2013.2255855)

[6] Y. Dong, H. Toyao and T. Itoh, "Design and Characterization of Miniaturized Patch Antennas Loaded with Complementary Split-Ring Resonators," in IEEE Transactions on Antennas and Propagation, vol. 60, no. 2, pp. 772-785, Feb. 2012. (doi: 10.1109/TAP.2011.2173120)

[7] R. Rajkumar and K. U. Kiran, "A Metamaterial Inspired Compact Open Split Ring Resonator Antenna for Multiband Operation, " in Wireless Personal Communications, vol. 97, no. 1, pp. 951-965, 2017. (doi: 10.1007/s11277-017-4545-0)

[8] R. Rajkumar and U. K. Kommuri, " A Triangular Complementary Split Ring Resonator Based Compact Metamaterial Antenna for Multiband Operation, " in Wireless Personal Communications, vol. 101, no. 2, pp. 1075-1089, 2018. (doi: 10.1007/s11277-018-5749-7)

[9] R. Rajkumar and K. U. Kiran, " A Compact ACS-Fed Mirrored L-Shaped Monopole Antenna with SRR Loaded for Multiband Operation, " in Progress In Electromagnetics Research C, vol. 64, pp. 159-167, 2016. (doi: 10.2528/PIERC16031501)

[10] V. Rajeshkumar, R. Rengasamy, P. V. Naidu, and A. Kumar, "A compact meta-atom loaded asymmetric coplanar strip-fed monopole antenna for multiband operation," in AEU - International Journal of Electronics and Communications, vol. 98, pp. 241-247, 2019. (doi: 10.1016/j.aeue.2018.10.011)

[11] Chul-Soo Kim, Jun-Seok Park, Dal Ahn, and Jae-Bong Lim, "A novel 1-D periodic defected ground structure for planar circuits," in IEEE Microwave and Guided Wave Letters, vol. 10, no. 4, pp. 131-133, Apr 2000. (doi: 10.1109/75.846922)

[12] M. Yang, Z. N. Chen, P. Y. Lau, X. Qing and X. Yin, "Miniaturized Patch Antenna With Grounded Strips," in IEEE Transactions on Antennas and Propagation, vol. 63, no. 2, pp. 843-848, Feb. 2015. (doi: 10.1109/TAP.2014.2382668)

[13] J. Pei, A. G. Wang, S. Gao, and W. Leng, "Miniaturized Triple-Band Antenna With a Defected Ground Plane for WLAN/WiMAX Applications," in IEEE Antennas and Wireless Propagation Letters, vol. 10, pp. 298-301, 2011. (doi: 10.1109/LAWP.2011.2140090)

[14] Mohammed Lamsalli, Abdelouahab El Hamichi, Mohamed Boussouis, Naima Amar Touhami, and Tajeddin Elhamadi, "Genetic Algorithm Optimization for Microstrip Patch Antenna Miniaturization," in PIER Lettors, Vol. 60, pp. 113-120, 2016. (doi:10.2528/PIERL16041907)

[15] Taiwo Olawoye and Pradeep Kumar, "A High Gain Antenna with DGS for Sub-6 GHz 5G Communications," in Advanced Electromagnetics, vol. 11, pp. 41-50, 2022.

[16] Ajithra.S, Maheswari.A, Vidhusharani.R, and Dr.C.Balamurugan, " Swastik Slotted Microstrip Patch Antenna For C Band Wireless Applications," in Advanced Electromagnetics, vol. 45, pp. 1514-1520, 2024.

[17] Ahmed Boutejdar, Mouloud Challal, Faiza Mouhouche, Kahina Djafri, and Saad Dosse Bennani, " Design and Fabrication of a Novel Quadruple-Band Monopole Antenna Using a U-DGS and Open-Loop-Ring Resonators," in Advanced Electromagnetics, vol. 6, pp. 59-63, 2017.

[18] Hesham A. El-Hakim and Hesham A. Mohamed, " Engineering planar antenna using geometry arrangements for wireless communications and satellite applications," in Advanced Electromagnetics, vol. 13, 2023.

[19] Doae El Hadri, Asmaa Zugari, Alia Zakriti and Mohssine El Ouahabi, " Dual-Band MIMO Antenna with Four CPW Elements using Polarization Diversity for 5G Mobile Communication Networks and Satellite," in Advanced Electromagnetics, vol. 12, pp. 43-53, 2023.